

The ESO Nearby Abell Cluster Survey^{*,**}

XI. Segregation of cluster galaxies and subclustering

A. Biviano¹, P. Katgert², T. Thomas², and C. Adami³

¹ INAF, Osservatorio Astronomico di Trieste, Italy

² Sterrewacht Leiden, The Netherlands

³ Laboratoire d'Astrophysique de Marseille, France

Received 22 October 2001 / Accepted 30 January 2002

Abstract. We study luminosity and morphology segregation of cluster galaxies in an ensemble cluster built from 59 rich, nearby galaxy clusters observed in the ESO Nearby Cluster Survey (ENACS). The ensemble cluster contains 3056 member galaxies with positions, velocities and magnitudes; 96% of these also have galaxy types. From positions and velocities we identify galaxies within substructures, viz. as members of groups that are significantly colder than their parent cluster, or whose average velocity differs significantly from the mean.

We compare distributions of projected clustercentric distance R and relative line-of-sight velocity v , of galaxy subsamples drawn from the ensemble cluster, to study various kinds of segregation, the significance of which is obtained from a 2-dimensional Kolmogorov-Smirnov test. We find that luminosity segregation is evident only for the ellipticals that are outside (i.e. not in) substructures and which are brighter than $M_R = -22.0 \pm 0.1$. This is mainly due to the brightest cluster members at rest at the centre of the cluster potential.

We confirm the well-known segregation of early- and late-type galaxies. For the galaxies with $M_R > -22.0$ of all types (E, S0, S and emission-line galaxies, or ELG, for short), we find that those within substructures have (R, v) -distributions that differ from those of the galaxies that are not in substructures. The early and late spirals (Sa-Sb and Sbc-Ir respectively) that are not in substructures also appear to have different (R, v) -distributions. For these reasons we have studied the segregation properties of 10 galaxy subsamples: viz. E, S0, S_e, S₁ and ELG, both within and outside substructures.

Among the 5 samples of galaxies that are *not in substructures*, at least 3 ensembles can and must be distinguished; these are: [E+S0], S_e, and [S₁+ELG]. The [E+S0] ensemble is most centrally concentrated and has a fairly low velocity dispersion that hardly varies with radius. The [S₁+ELG] ensemble is least concentrated and has the highest velocity dispersion, which increases significantly towards the centre. The class of the S_e galaxies is intermediate to the two ensembles. Its velocity dispersion is very similar to that of the [E+S0] galaxies in the outer regions but increases towards the centre.

The galaxies *within substructures* do not all have identical (R, v) -distributions; we need to distinguish at least two ensembles, because the S0 and [S₁+ELG] galaxies have different distributions in R as well as in v . The [S₁+ELG] galaxies are less centrally concentrated and, in the inner region, their velocity dispersion is higher than that of the S0 galaxies. Our data allow the other 3 galaxy classes to be combined with these two classes in 4 ways.

We discuss briefly how our data provide observational constraints for several processes inside clusters, like the destruction of substructures, the destruction of late spirals and the transformation of early spirals into S0s.

Key words. galaxies: clusters: general – galaxies: elliptical and lenticular, cD – galaxies: evolution – galaxies: kinematics and dynamics – cosmology: observations

1. Introduction

It has been known for a long time that in clusters, galaxies of different classes have different projected distributions. Oemler (1974), Melnick & Sargent (1977) and

Dressler (1980) were the first to quantify these differences. Dressler (1980) showed that the different distributions arise mainly from the so-called morphology-density relation (MDR): i.e., the relative fractions of ellipticals, S0s and spirals correlate very well with local surface density. Hence, the composition of the galaxy population changes with distance from the cluster centre.

Postman & Geller (1984) derived an MDR over 6 decades of local space density from the CfA redshift survey, and in the Pisces-Perseus supercluster – and in

Send offprint requests to: A. Biviano,
e-mail: biviano@ts.astro.it

* Based on observations collected at the European Southern Observatory (La Silla, Chile).

** <http://www.astrsp-mrs.fr/www/enacs.html>

particular in its long filament – Giovanelli et al. (1986) found a clear MDR. In this supercluster, even early and late spirals have different distributions, and this was also found for spirals in groups of galaxies (Giuricin et al. 1988). The MDR was also studied in several individual nearby clusters (e.g. Andreon 1994, 1996; Caon & Einasto 1995) and in general redshift surveys (e.g. Santiago & Strauss 1992).

In spite of the wealth of observational data, it is still not totally clear how the MDR arises. In clusters, galaxy encounters must play a rôle, so that gas-rich disk galaxies cannot survive in the dense cores of clusters. Contrary to Dressler (1980), Whitmore & Gilmore (1991) and Whitmore et al. (1993) found that morphological fraction correlates as tightly with clustercentric distance as with projected density. An explanation for the MDR in a cold dark matter-dominated universe was given by Evrard et al. (1990).

The study of the MDR was extended towards higher redshifts, e.g. by Dressler et al. (1997), Couch et al. (1998) and Fasano et al. (2000), and was linked to the more general question of the evolution of galaxies in environments of different densities (e.g. by Menanteau et al. 1999). Dressler et al. (1997) found that the regular, centrally concentrated clusters at a redshift of about 0.5 show a strong MDR, as do the low-redshift clusters. However, the less concentrated and irregular clusters at $z \approx 0.5$ do not show a clear MDR, unlike their low-redshift counterparts.

Dressler et al. also noted that the fraction of S0s appears to decrease quite strongly with increasing redshift (by as much as a factor of 3 from $z = 0$ to $z \approx 0.5$), and Fasano et al. (2000) studied this effect in clusters at redshifts between 0.1 and 0.25. The reality of this decrease was questioned by Andreon (1998) who argued that it is not trivial to establish a reliable elliptical/S0-ratio. Also, the elliptical/S0-ratio may not be very meaningful (even if it can be established accurately) because the differences between ellipticals and S0s may not be major (e.g. Jørgensen & Franx 1994).

Morphological segregation in position is often accompanied by morphological segregation in velocity space, i.e. galaxies of different types have different velocity dispersions, or velocity dispersion profiles (e.g. Tamman 1972; Moss & Dickens 1977; Sodré et al. 1989; Biviano et al. 1992). The effect is sometimes reported as a correlation between kinematics and colours (e.g. Colless & Dunn 1996; Carlberg et al. 1997a).

Luminosity segregation was detected by Rood & Turnrose (1968), Capelato et al. (1981), Yepes et al. (1991) and Kashikawa et al. (1998). Luminosity segregation was detected both as a segregation in clustercentric distance, and as a kinematical segregation, viz. the most luminous galaxies have the smallest velocity dispersion (see e.g. Rood et al. 1972). Yet, kinematical segregation appears to occur mostly (Biviano et al. 1992), if not exclusively (Stein 1997), for ellipticals, and much less – if at all – for the other galaxy types. Fusco-Femiano & Menci (1998)

explained the observed degrees of luminosity segregation by their merging models.

Adami et al. (1998a) studied a sample of about 2000 galaxies in 40 nearby Abell clusters and confirmed that the overall velocity dispersion depends on galaxy type, and increases along the Hubble sequence. The velocity dispersion profiles for the various galaxy types indicate that the spirals may not yet be fully virialized, and may still be mostly on radial, infalling orbits. The spirals may thus have properties similar to the galaxies with emission lines (ELG), which were studied in A576 by Mohr et al. (1996), and by Biviano et al. (1997, hereafter Paper III) in the clusters observed in the ESO Nearby Abell Cluster Survey (ENACS). Biviano et al. concluded that the ELG probably have a significant velocity anisotropy. De Theije & Katgert (1999, hereafter Paper VI) distinguished early- and late-type galaxies in the ENACS from their spectra, and concluded that the evidence for radial orbits was only significant for the ELG.

Recently, Thomas (2002, hereafter Paper VIII) derived morphologies for close to 2300 ENACS galaxies from CCD imaging. By adding morphologies from the literature, and spectral types from the ENACS spectra, this provides essentially complete type information for the galaxies in a sample of 59 ENACS clusters. This dataset allows a vastly improved analysis of the distribution and kinematics of the various classes of galaxies in clusters, which we present in this paper. In a subsequent paper (Katgert et al. 2002) we derive the mass profile of the ENACS clusters.

In Sect. 2 we summarize the data that we used. In Sect. 3 we discuss the method by which we study the various types of segregation. In Sect. 4 we discuss the effect of substructure and in Sects. 5 and 6 we discuss the evidence for luminosity and morphology segregation, as well as the minimum number of galaxy ensembles that must be distinguished. In Sect. 7 we discuss the nature of the morphological segregations and in Sect. 8 we discuss the implications of our results for ideas about cluster galaxy evolution. In Sect. 9 we present a summary and the main conclusions.

2. The data

We use data from the ENACS (see Katgert et al. 1996 – Paper I – and Katgert et al. 1998 – Paper V). We have imposed a redshift limit of $z < 0.1$ and we applied a lower limit of 20 to the number of member galaxies; this defines a sample of 67 clusters that is essentially volume-limited (Mazure et al. 1996 – Paper II). Clusters were defined in redshift space, from the distribution of the line-of-sight velocities. We used a density-dependent gap (Adami et al. 1998b) rather than a fixed gap (as was used in Paper I) to accommodate different total numbers of galaxies. The membership of the ENACS clusters with at least 20 redshifts hardly changes when we use a variable instead of a fixed gap.

Interlopers (non-members, seen in projection onto the cluster) were eliminated with the interloper removal

procedure devised by den Hartog & Katgert (1996). For the systems with at least 45 galaxies with redshifts ($N_z \geq 45$) we calculated an “interim” mass profile. This predicts the maximum line-of-sight velocity at the projected position of each galaxy from which we determine if the galaxy can be within the turn-around radius. This procedure was repeated until it converged. For clusters with $N_z \lesssim 45$, such a procedure generally does not work; therefore we used for them the separation between members and interlopers as defined in a statistical manner by the $N_z \geq 45$ clusters (for details, see Katgert et al. 2002).

Our magnitudes are R -band, and the absolute magnitudes, M_R , were derived for $H_0 = 100 \text{ km s}^{-1} \text{ Mpc}^{-1}$, with K-corrections according to Sandage (1973) and corrections for galactic absorption according to Burstein & Heiles (1982). For the galaxies in our sample, these corrections are quite small, viz. ~ 0.1 mag. Information on galaxy type comes from various sources: either from a CCD image (mostly from Paper VIII), or from the ENACS spectrum (using a Principal Component Analysis in combination with an Artificial Neural Network, see Paper VI). A comparison of the various type estimates and a discussion of their robustness is given in Paper VIII. Several hundred galaxies have one or more emission lines in their ENACS spectrum (we refer to those as ELG, see Paper III). Most of these ELG have narrow lines due to warm gas.

The galaxies with type information were assigned to the following classes: ellipticals (E), S0, spirals (S), and the intermediate classes, E/S0, and S0/S. Whenever possible, we also distinguished between early (S_e) and late (S_l) spirals, i.e., spirals with type earlier than or as early as Sb, and later than Sb, respectively. The classes E, S0, S and ELG are “pure” and “exclusive”: i.e. the E, S0 and S do not contain ELG; as a matter of fact we ignored the ELG in Es and S0s. The class E/S0 is not used separately, but it is included in the class of early-type galaxies, together with E and S0, when these two classes are linked in one sample (see Sect. 6). The S0/S class was never used. In clusters where galaxy types could only be estimated from spectra, the pure E class does not occur and the “earliest” galaxy class is E/S0 (see also Paper VIII). Similarly, early and late spiral galaxies can only be classified on CCD images. However, late spirals can be recognized from the spectrum alone (see Paper VIII).

We considered including galaxies and clusters with non-ENACS data, but segregation can only be studied usefully for data with a sufficiently uniform completeness limit in apparent magnitude. For literature data this requirement often is not met, so *literature data were not used to enlarge the ENACS galaxy samples*; we only used *galaxy types* from the literature if there was no ENACS galaxy type. Redshifts from the literature were only used in the identification of interlopers in the ENACS galaxy samples.

The analysis of the distribution and kinematics of the various galaxy classes can only be done for clusters with galaxy types for a sufficiently high fraction of the galaxies, and we required this fraction to be at least 0.80. This

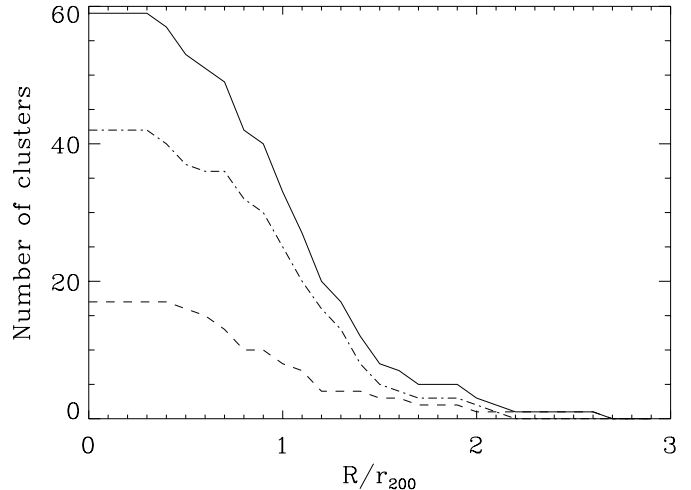


Fig. 1. The number of clusters contributing to the analysis, as a function of R/r_{200} , for the various galaxy classes. The full-drawn line refers to all 59 clusters, the dashed line to the 17 clusters with only spectral galaxy types (i.e. no pure E-type nor S_e), and the dot-dashed line to the 42 clusters with CCD imaging (i.e. with all galaxy types).

defines a sample of 59 ENACS clusters with $z < 0.1$; all clusters have 20 or more ENACS member galaxies, for at least 80% of which a galaxy type is known. The total number of galaxies in the 59 clusters is 3056, and for 2948 (96%) of those a galaxy type is known. In the sample of 59 clusters, there are 429 ELG, i.e. galaxies with one or more emission lines in the spectrum. Information about the 59 clusters is given in Appendix A.

Combination of data in clusters of various sizes and masses into an ensemble cluster requires that projected distances and relative velocities (or rather, their line-of-sight components) are properly scaled. Projected distances R were scaled with r_{200} , the radius within which the average density is 200 times the critical density of the universe and which is very close to the virial radius. We assumed, like Carlberg et al. (1997b), that $M(< r) \propto r$, so that r_{200} follows from the global value of the dispersion of the line-of-sight component of the velocities, σ_p ; viz. $r_{200} \approx \sqrt{3} \sigma_p / (10 H(z))$, with $H(z)$ the Hubble parameter at redshift z . The line-of-sight components ($v - \bar{v}$) of the relative velocities of the galaxies were scaled with the global velocity dispersions σ_p of the parent cluster. Note that σ_p was calculated for all galaxies together, irrespective of type, so that the relative velocities of the *different types of galaxies* are all normalized by the *same overall velocity dispersion*. For the clusters in Table A.1 the average value of σ_p is about 700 km s^{-1} , so that the average value of r_{200} is about $1.2 h^{-1} \text{ Mpc}$.

In Fig. 1 we show the number of clusters contributing in the various R/r_{200} -intervals (solid line). Also shown are the numbers for the clusters with only spectral galaxy types (i.e. that do not have E- and S_e -types), and clusters with CCD-imaging (that have all types).

3. Detecting segregation

Segregation, i.e., the fact that the various galaxy populations have different phase-space distributions, may show up either in the projected distribution, or in the kinematics, or in both. In order to use our data optimally, we searched for the various types of segregation by comparing (R, v) -distributions in an unbinned way, using the combined evidence from projected positions and relative velocities. Luminosity and morphology segregation are generally presented through compression of (R, v) -distributions, i.e., through projection onto the R - or the v -axis. Luminosity and morphology segregation are thus often referred to as “kinematical segregation” with respect to magnitude or morphology. However, it is important to consider radial and kinematical segregation together, because they may not be independent.

We use an ensemble cluster constructed from the 59 ENACS clusters listed in Table A.1. From this ensemble cluster we select various galaxy subsamples. Combination of the 59 clusters is necessary to have the best “signal/noise”. However, the implicit assumption is that the distributions of the various galaxy type and magnitude subsamples are sufficiently similar in the individual clusters, or in different classes of clusters, so that their combination is meaningful. This is not guaranteed, as cosmic variance is not negligible. It is therefore possible, if not likely, that no real cluster is described satisfactorily by the ensemble cluster; however, the ensemble cluster gives the best picture that we have of an average rich nearby cluster.

For the estimate of the projected clustercentric distance R , it is important that the determination of the centre of the parent cluster is as unbiased as possible. We have taken special care that the centres of all clusters are determined with similar methods, and with sufficient accuracy. For the calculation of the centre position we followed the procedure described in Paper III: in order of decreasing preference we used the X-ray centre, the brightest cluster member in the core of the cluster, the peak in the galaxy surface density (if necessary luminosity-weighted) or the biweight average (e.g., Beers et al. 1990) of all galaxy positions to derive the central position. The estimated accuracy that can be obtained in this way is 50–60 kpc (see also Adami et al. 1998c). The positions of the adopted cluster centres are given in Table A.1 in Appendix A.

The advantage of comparing (R, v) -distributions is that structure in the (R, v) -distribution is not diluted in projection onto either the R - or v -axis. However, as a result of the generally non-circular shapes of the apertures in which the ENACS redshift surveys of the clusters were done (see, e.g., Fig. 10 in Paper I), the distribution in projected radial distance is always biased. We estimate this radial bias by assuming circular symmetry for the cluster galaxy distributions, knowing the positions (and size) of the Optopus plates that were used to sample the clusters (see Fig. 10 in Paper I). Another source of radial bias arises from the fact that we stack clusters which have been

sampled out to different apertures. Selection of different morphological types sometimes results in the selection of a subsample of the original 59 clusters (Fig. 1). Different cluster subsamples have different degrees of incompleteness at a given radius. We estimate this radial bias by using an approach similar to that adopted by Merrifield & Kent (1989).

When comparing two (R, v) -distributions one must either ensure that these biases are identical, or take the differences in the biases into account before making the comparison. Since galaxy subsamples can have different radial distributions, the fact that clusters have been sampled out to different radii may be a complicating factor. For *all* KS2D comparisons presented in this paper, the radial biases in the two (R, v) -distributions were found to be either identical, or so similar that a straight comparison was justified.

The number of clusters that contribute to the ensemble clusters of the various galaxy types, at various projected radial distances, is shown in Fig. 1. In order to ensure that an ensemble cluster is sufficiently representative (i.e. is built from a sufficient number of clusters) we have always compared (R, v) -distributions over the radial range $0 \leq R/r_{200} \leq 1.5$. This means that the ensemble cluster includes at least 13 out of 59 clusters (or 9 out of 45, for E and for S_e).

The actual comparison of two (R, v) -distributions was done with the 2-D version of the Kolmogorov-Smirnov test (KS2D, for short), as described by Peacock (1983) and Fasano & Franceschini (1987). The Kolmogorov-Smirnov (KS) test is relatively conservative: if it indicates that two distributions have a high probability of not being drawn from the same parent population, other tests (e.g. Rank-Sum tests or Sign Tests) indicate the same. However, the KS test does not always support differences indicated by other tests. Therefore, even if the number of galaxies in one or both of the samples is relatively small, a small probability for the samples to be drawn from the same population in general is trustworthy. However, if the difference is not significant, this *does not prove* that the two samples are drawn from the same parent population, because real differences can be made undetectable by limited statistics.

We checked the performance of the KS2D test by randomly assigning half of the galaxies in each cluster to one of two ensemble clusters, each comprising half the total number of galaxies in the ensemble cluster built from the 59 clusters. According to the KS2D-test the probability that the two subsets are drawn from the same parent distribution is 83%. This is fully consistent with the fact that they were drawn from the same parent distribution and that there are no differences between them other than statistical fluctuations.

4. The effect of substructure

The combination of data for many clusters into an ensemble cluster is unavoidable, especially because galaxy

subsamples in individual clusters are too small for segregation studies. However, combining clusters in an ensemble cluster inevitably reduces the relative amplitude of substructure. Because substructure may play an important rôle in the formation and evolution of clusters, we have estimated the effect of substructure on the kinematics and distribution of the various galaxy classes, in two ways. First, we compared clusters with and without *global* substructure, and secondly we compared galaxies that reside in and outside *local* substructures in their respective clusters.

4.1. Clusters with and without substructure

Because substructure may take different forms, different filters are required (and have been devised) for its detection. A general problem for the detection is that observations only provide the 2+1-D projected version of the 3+3-D phase-space, which reduces the detectability. We have used a slightly modified version of the test devised by Dressler & Schectman (1988). This test is sensitive to spatially compact subsystems that either have an average velocity that differs from the cluster mean, or have a velocity dispersion that differs from the global one, or both.

For each galaxy we selected the n_{loc} neighbours that are closest in projection, where n_{loc} was taken to be $\sqrt{N_{\text{mem}}}$ (see, e.g., Bird 1994) with N_{mem} the total number of cluster members with redshifts. For these n_{loc} neighbours we calculated the average velocity, \bar{v}_{loc} and the velocity dispersion σ_{loc} . From these parameters, we calculated for each galaxy a quantity δ , designed to indicate groups (of n_{loc} members) that are “colder” than the cluster and/or have an average velocity that differs from the global cluster mean.

The parameter δ was calculated as follows:

$$\delta = \frac{1}{\sigma_p(R)} \sqrt{\frac{n_{\text{loc}} \delta_v^2}{[t_{n_{\text{loc}}-1}]^2} + \frac{\delta_\sigma^2}{\left[1 - \sqrt{(n_{\text{loc}} - 1)/\chi_{n_{\text{loc}}-1}^+}\right]^2}} \quad (1)$$

with $\delta_v = |\bar{v}_{\text{loc}} - \bar{v}_{\text{glob}}|$, and $\delta_\sigma = \max(\sigma_p - \sigma_{\text{loc}}, 0)$, where the Student- t and χ^2 distributions are used to calculate the uncertainty in the velocity and velocity-dispersion differences, respectively. To suppress noise, we finally calculated δ for each galaxy as the average of the δ -values of its $n_{\text{loc}} - 1$ neighbours. The larger the value of δ the larger the probability that the galaxy finds itself in a moving and/or cold subgroup within its cluster.

As shown in Paper III, at least 40–50 galaxies are needed for a decision about whether a cluster contains significant substructure or not. In Table 1 we list the results for the 23 clusters with at least 45 members. For each cluster a global Δ parameter was calculated as the sum of the individual δ 's of all galaxies. The observed value of Δ was compared with the 1000 Δ values obtained in 1000 random azimuthal scramblings of the galaxy positions of the same cluster. In the scramblings the incomplete azimuth coverage was taken into account. The fraction of scramblings with a value of Δ larger than the observed one is

Table 1. The evidence for substructure in the clusters with at least 45 members with ENACS redshifts.

ACO	\bar{v}_{3K} km s ⁻¹	ENACS		P_Δ	σ_p km s ⁻¹
		z	type		
119	12997	102	87	0.917	720
168	13201	76	71	0.305	518
514	21374	82	74	0.684	875
548	12400	108	108	0.005	710
548	12638	120	116	0.000	824
978	16648	56	52	0.081	497
2734	18217	77	77	0.010	579
2819	22285	49	44	0.778	409
3094	20027	66	64	0.000	654
3112	22417	67	60	0.211	954
3122	19171	89	88	0.000	782
3128	17931	152	152	0.000	765
3158	17698	105	102	0.771	1006
3223	17970	66	65	0.204	597
3341	11364	63	63	0.569	561
3354	17589	56	56	0.008	367
3558	14571	73	73	0.063	1035
3562	14633	105	105	0.000	903
3651	17863	78	78	0.019	662
3667	16620	103	102	0.151	1037
3806	22825	84	83	0.600	808
3822	22606	84	68	0.079	971
3825	22373	59	57	0.106	699

the probability P_Δ that the observed value is due to noise, and thus not indicative of real substructure. Thus, a low value of P_Δ indicates a high probability of significant substructure.

There are 9 clusters with $P_\Delta \leq 0.05$, i.e. with significant global substructure, and these contain 851 galaxies. The other 14 clusters, containing 1069 galaxies, have $P_\Delta > 0.05$, i.e. are without significant global substructure. The average number of galaxies in the substructure clusters is higher than it is in the non-substructure clusters (95 against 76). This is a reminder that some of the non-substructure clusters may have substructure that was not detected due to limited statistics. There is no relation between the presence of substructure and global velocity dispersion: the 9 substructure clusters have an average velocity dispersion of 694 ± 52 km s⁻¹, for the 14 clusters without substructure this is 763 ± 59 km s⁻¹.

A KS2D comparison of the (R, v) -distributions of the total galaxy populations in substructure and non-substructure clusters shows that the two samples have a probability of <0.1% to have been drawn from the same parent sample. This forces us to analyze the segregation properties of galaxies within and outside substructures separately.

4.2. Galaxies in and outside substructures

Instead of summing all individual values of δ to get a measure of the amount of substructure in the cluster as a whole (as was done in Sect. 4.1), one can also use the

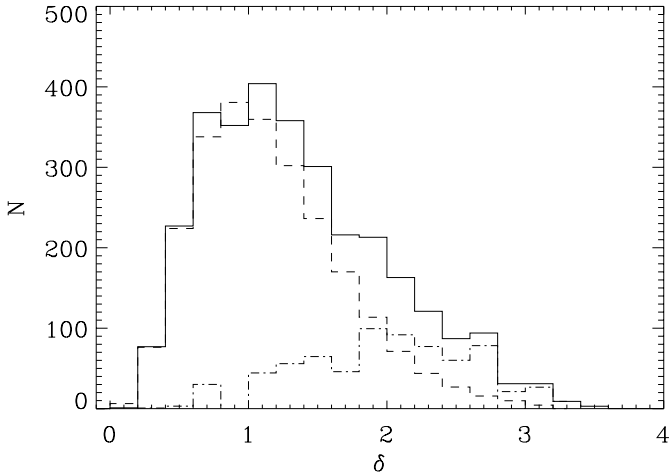


Fig. 2. The distribution of the substructure parameter δ for the 3056 galaxies in the 59 clusters. The solid line represents the observations, the dashed line the distribution for the azimuthally scrambled clusters (normalized to the observed number with $\delta < 1$), and the dash-dotted line gives the difference between the two.

individual δ -values to select galaxies in significant local substructures in their cluster. In other words: whereas in Sect. 4.1 *all* galaxies in a cluster were made to follow the classification of their cluster, one may also consider all galaxies in significant local substructures, independent of the classification of the parent cluster. Even in clusters without significant *global* substructure, some galaxies may be in *local* substructures. Similarly, in clusters with significant substructure, not all galaxies are in local substructures.

In Fig. 2 we show the distribution of δ for all 3056 galaxies in the 59 clusters in our sample. In order to use δ to select galaxies in and outside cold and/or moving groups, we must determine the value of δ that optimally separates them. To that end, we azimuthally scrambled the galaxy distributions, taking into account the incomplete azimuth coverage due to the generally non-circular shapes of the apertures within which the ENACS spectroscopy was done. The resulting distribution of δ (the dashed line in Fig. 2) was normalized to produce the observed numbers of galaxies with $\delta < 1.0$.

This normalization was chosen because for $\delta < 1.0$ no significant contribution of galaxies in substructures is expected. This is borne out by the fact that the observed and scrambled δ -distribution have essentially the same shape for $\delta < 1.0$. The difference between the observed and scrambled δ -distributions gives the distribution of the galaxies that presumably are in substructures (the dash-dotted line in Fig. 2). The galaxies that are not in substructures can be selected quite satisfactorily by requiring $\delta < 1.8$. Both the completeness and reliability of that sample of 2304 galaxies are very close to 90%. We will therefore define all (sub-)samples of galaxies not in substructures with an upper limit in δ of 1.8.

The lower limit in δ for the selection of galaxies within substructures is less obvious. Using $\delta > 1.8$, the completeness and reliability of the substructure-sample (of 752 galaxies) are both about 65%. I.e., one in three of the galaxies with $\delta > 1.8$ is *not* in substructures. Increasing the lower limit in δ to reduce the contamination by galaxies outside substructures also reduces the number of galaxies in substructures available for the tests. For comparisons of (R, v) -distributions involving samples of galaxies in substructures, we therefore always defined 4 parallel samples, with $\delta > 1.8, 2.0, 2.2$ and 2.4 to vary the balance between contamination and statistical weight. If the results for those 4 samples are identical, contamination is not important; otherwise the 4 results must be interpreted.

We made a KS2D comparison of the (R, v) -distributions of the total galaxy populations within and outside substructures, using $\delta > 1.8$ for the substructure sample. The probability that the (R, v) -distributions of the two samples are drawn from the same parent distribution is very small, viz. again $< 0.1\%$.

4.3. Characteristics of the substructures

The definition of substructures that we used was designed to select cold and/or moving groups. However, because the membership of a group is fixed to be n_{loc} , the properties of the groups are not necessarily constant. E.g., the “size” of a group depends on n_{loc} and on the surface density of galaxies, which in turn depends on the redshift sampling of the cluster N_{mem} , so that the groups in different clusters may have different sizes. This disadvantage is outweighed by the fact that by setting $n_{\text{loc}} = \sqrt{N_{\text{mem}}}$ one maximizes the sensitivity to significant substructures while reducing the sensitivity to Poisson noise (e.g. Silverman 1986). The latter is important, as in our clusters n_{loc} is never as high as the optimum value of ≈ 25 , derived by Knebe & Müller (2000) from an analysis of simulated clusters.

However, even within a cluster the “size” of the selected groups is not constant, but varies with distance from the centre because the surface density increases noticeably towards the centre. This effect is clearly visible in our data: the harmonic mean radius of the $n_{\text{loc}} - 1$ neighbours increases with projected distance from the cluster centre. One could avoid this bias by choosing a fixed physical scale for the selected subclusters. However, if the scale is chosen large enough for a reasonable number of galaxies to be selected at large radii, substructures in the central region would be averaged out.

Using the δ -values of the individual galaxies, we have attempted to identify “subclusters” as follows. First, we selected all galaxies in each cluster with a value of $\delta > \delta_{\text{lim}}$. Then we calculated the harmonic mean projected radius and the velocity dispersion of the group of n_{loc} nearest neighbours around each of these galaxies. These groups were subsequently merged if both their projected distance was less than the sum of their harmonic mean radii, and the difference of their average velocities was less

than the mean of their velocity dispersions. The resulting “subclusters” consist of all galaxies with $\delta > \delta_{\text{lim}}$ in the groups from which they were built.

For $\delta_{\text{lim}} = 2.0$ we find 62 subclusters in the 59 clusters, i.e. on average one per cluster. The mean number of galaxies with $\delta > 2.0$ in a subcluster is 8.6, and individual numbers go up to about 60 (in the very rich cluster A3128). Note that 16 clusters do *not* have a subcluster, while some subclusters are found in clusters that do not show significant evidence for substructure with the test of Dressler & Schectman. Note also that, while the harmonic mean radius of the selected “subclusters” is observed to increase with clustercentric distance, their velocity dispersion stays remarkably constant at $\sigma_{\text{loc}} \sim 400\text{--}500 \text{ km s}^{-1}$.

The filter that we used will not have detected all galaxies that belong to substructures. Yet, as shown by our azimuthal scramblings, a large fraction of those that *are* selected, *do* belong to subclusters (where this fraction obviously increases with increasing lower limit in δ). The galaxies selected to be in subclusters do not form a complete sample, but we treat them as a distinct class, if only because their (R, v) -distribution is likely to be influenced by the fact that they are dynamically linked in subclusters. This is actually confirmed by the results of the KS2D tests described in Sect. 4.2.

From histograms like those in Fig. 2 in several radial intervals, we conclude that the δ -distribution of galaxies in substructures, corrected for accidental substructure through azimuthal scrambling (the dashed-dotted line in Fig. 2), does not vary significantly with radius. Therefore, we felt justified to apply radius-independent δ -cuts for galaxies inside and outside of substructures.

With our normalization of the δ -distribution of the azimuthally scrambled clusters (see Fig. 2), the average fraction of galaxies in substructures, corrected for accidental substructure, is 0.22. However, this fraction appears to depend on the central concentration of the galaxy distribution. We quantify the latter by a concentration index, calculated as the ratio of the number of galaxies within $0.25 r_{200}$, and between 0.25 and $0.50 r_{200}$. This index is not affected by azimuthal incompleteness (Sect. 3) because that is negligible within $0.50 r_{200}$. The 23 clusters with high concentration index contain 1527 galaxies, the 36 low-concentration clusters contain 1529 galaxies. The corrected fractions of galaxies in substructures in the two cluster samples are 0.17 ± 0.01 and 0.27 ± 0.01 respectively. In other words: in clusters with low central concentration the fraction of galaxies in substructures is significantly higher than in clusters with high central concentration. Such a correlation is also seen in numerical cosmological simulations (Thomas et al. 2001).

The number of galaxies in substructures also appears to decrease markedly towards the centre. This is shown in the upper panel of Fig. 3 which gives the radial distribution for the galaxies with $\delta > 2.2$ (similar results are obtained for other values of δ_{lim}). The solid line is the observed distribution, the distribution in the azimuthally scrambled clusters is given by the dashed line, while the

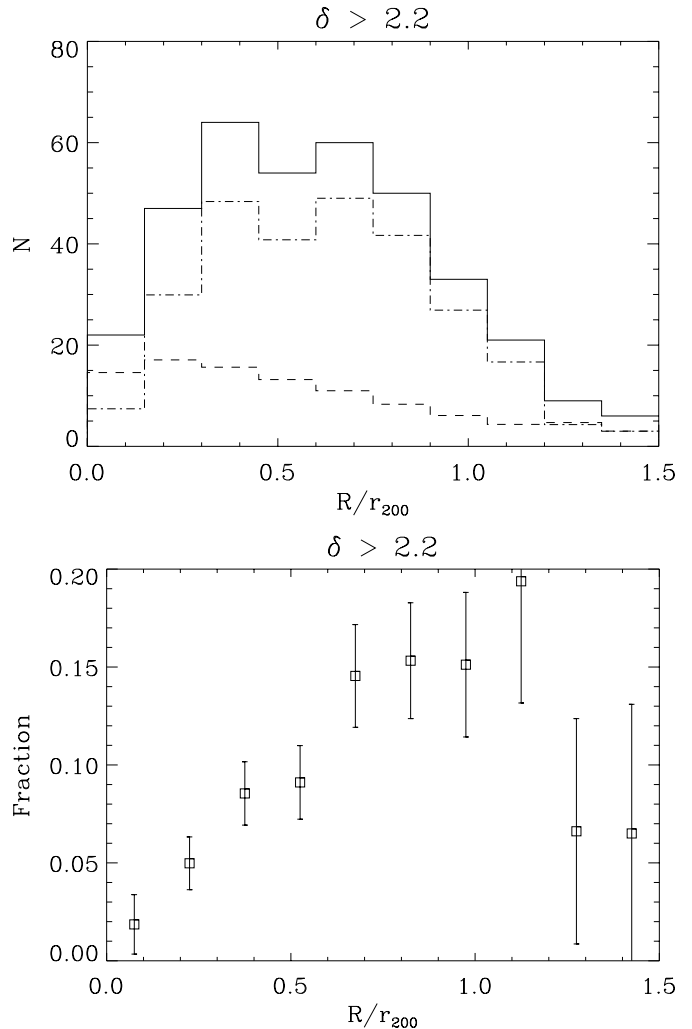


Fig. 3. Top: the distribution of the galaxies with $\delta > 2.2$ in the 59 clusters, as a function of projected radius R . The solid line represents the observed distribution, the dashed line the distribution for the azimuthally scrambled clusters, while the dash-dotted line gives the difference between the two. Bottom: the fraction of galaxies in substructures, with $\delta > 2.2$, as a function of projected radius R .

dash-dotted line is the difference between the two. The latter is a reliable estimate of the radial distribution of galaxies in substructures. In the lower panel of Fig. 3 we show the fraction of galaxies in substructures, with $\delta > 2.2$, with respect to the total number of galaxies. The most remarkable feature in Fig. 3 is the very strong and abrupt decrease for $R \leq 0.3 r_{200}$ of the number of galaxies really in substructures (the dash-dotted line in the upper panel).

One might wonder to what extent the strong decrease of the number of galaxies in substructures within $R \approx 0.3 r_{200}$ could, at least partially, be caused by a selection effect. As we discussed above, the “size” of the substructures selected by our “filter” is smaller in the centre than it is at the periphery. Therefore, we are insensitive to substructures with a large linear scale in the centre, and to small-scale substructures in the periphery. Whereas small-scale substructures might exist

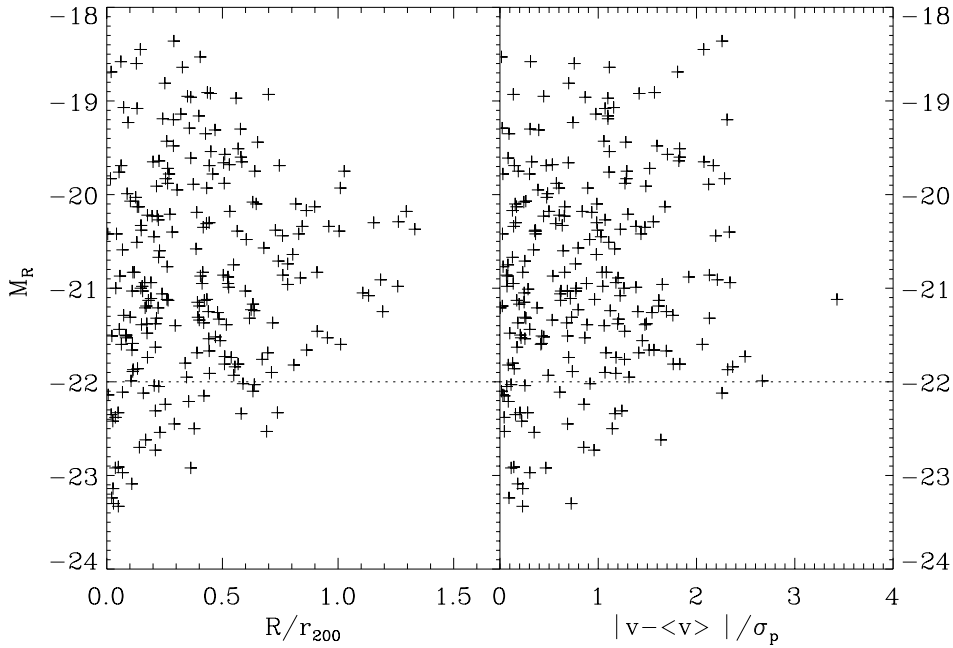


Fig. 4. The relations between absolute magnitude and projected radial distance (left) and normalized relative velocity (right) for ellipticals outside substructures.

in the periphery, it is unlikely that in the central region large-scale substructures, could have survived, if they existed. As was shown by González-Casado et al. (1994), the less massive subclusters are tidally disrupted in one cluster crossing, while the more massive clumps migrate towards the centre through dynamical friction and disappear as substructure. Therefore, we believe that the strong decrease of the number of galaxies in substructures towards the centre is real. The effect is reminiscent of the almost total absence of binary galaxies in the inner region of rich clusters ($R \lesssim 0.4 h^{-1}$ Mpc), discussed by den Hartog (1997).

5. Luminosity segregation

Evidence for luminosity segregation (LS) is generally presented as a dependence on magnitude of the distribution of intergalaxy distances, i.e., of the angular correlation function of the galaxies. The global character of LS is that the brightest galaxies have a more central distribution than the other galaxies. As an extreme example, the brightest galaxies (frequently cDs) are found very close to the cluster centre. However, not all clusters that have been studied for LS do show evidence for it.

A robust detection of LS requires a large number of member galaxies. In several cases, field galaxies are included in the analysis as no redshifts are available, and those are then a source of noise (see e.g. Yepes et al. 1991; Kashikawa et al. 1998). In the ENACS, field galaxies were eliminated quite well, but the number of member galaxies in most of the clusters in Table A.1 is not sufficient to study LS in individual clusters. The ensemble of all 59 clusters does have sufficient statistical weight, but the

combination of many clusters may dilute real LS in (some of) the individual clusters.

We searched for LS with many KS2D tests in which we compared two (R, v) -distributions of the same class of galaxies, like ELG_{nosub} or $S0_{\text{sub}}$ etc., which differ only in the range of absolute magnitude. In other words: the parent sample of ELG_{nosub} or $S0_{\text{sub}}$ etc. was split in absolute magnitude at M_{cut} , the value of which we varied. For the galaxies in substructures we did the tests not only for several values of M_{cut} but also for the four lower limits in δ that we discussed in Sect. 4.2. All those tests show only one robust case of LS: namely for the ellipticals outside substructures. As elsewhere in this paper, differences are considered real only if there is less than 5% probability that two (R, v) -distributions are drawn from the same parent distribution. For the ellipticals outside substructures, we consistently get probabilities of less than 5% for all M_{cut} 's in the range -22.5 to -21.0 .

In Fig. 4 we show the relations between absolute magnitude and projected radial distance (left), and normalized relative velocity (right), for the ensemble cluster of ellipticals with $\delta < 1.8$. The brightest ellipticals have velocities close to the systemic velocity and are found mostly in the very centres of their parent clusters. The fact that the KS2D tests give a signal for a range of M_{cut} must be due to “cross-talk”: the segregation of the brightest ellipticals is so strong that it shows up even if fainter ellipticals are included. To estimate the value of M_{cut} that optimally separates the bright galaxies that show LS from the faint ones which do not, we have proceeded as follows.

The faint ellipticals with $-20.6 < M < -20.0$ were taken as a reference sample, presumably unaffected by LS. We compared the (R, v) -distribution of this reference

Table 2. The number of galaxies with $R/r_{200} \leq 1.5$ and $M_R > -22.0$ in each of the samples used.

gal type	outside substr.	within substructures			
		$\delta > 1.8$	$\delta > 2.0$	$\delta > 2.2$	$\delta > 2.4$
E	200	60	41	30	15
S0	795	261	176	114	70
S _e	183	63	41	28	21
S ₁	113	25	19	16	12
ELG	236	88	73	56	44
E/S0	165	72	51	36	19
S _{generic}	119	33	25	18	13

sample with that of the brighter ellipticals with $[M_{\text{cut}} - 0.25, M_{\text{cut}} + 0.25]$, for values of M_{cut} between -23.25 and -21.55 . The faintest M_{cut} for which the two samples are different is -22.0 , and we estimate that the uncertainty in this value is at least 0.1. In the following we adopt $M_R = -22.0$ as the absolute magnitude above which LS occurs for ellipticals. Although the KS2D tests do not show significant evidence for LS of galaxies other than the bright ellipticals, we decided to exclude galaxies of *all* types with $M_R < -22.0$ in the analysis of morphological segregation, to avoid possible cross-talk of low-level LS into morphological segregation.

We have investigated the relation between the brightest ellipticals and the 1st- and 2nd-ranked galaxies in the clusters as follows. Comparison of the (R, v) -distributions of these classes shows that 1st-ranked galaxies (or brightest cluster galaxies, BCGs) and the brightest ellipticals are not significantly different. On the contrary, those of the 2nd-ranked galaxies and the brightest ellipticals *are*, and this is also the case for the 1st- and 2nd-ranked galaxies. It is noteworthy that of the brightest ellipticals 15% are neither 1st-ranked nor 2nd-ranked galaxies. As a matter of fact, the average type of 1st-ranked galaxies is intermediate between E and S0, while that of the 2nd-ranked galaxies is S0.

6. Morphology segregation

6.1. Segregation results

We investigated the evidence for morphological segregation by means of a large number of KS2D comparisons. Because it turned out that the (R, v) -distributions of early and late spirals (S_e and S₁) that are *not in substructures* have less than 4% probability of being drawn from the same parent distribution, we did not consider them together. For the spirals *within substructures* there is no evidence that we must consider S_e and S₁; however, for consistency, we also treated them separately. We therefore made KS2D comparisons of the (R, v) -distributions of the following 10 galaxy classes: E_{nosub}, S0_{nosub}, S_{e, nosub}, S_{1, nosub}, ELG_{nosub}, E_{sub}, S0_{sub}, S_{e, sub}, S_{1, sub} and ELG_{sub}. The number of galaxies with $R/r_{200} \leq 1.5$ in each galaxy class is shown in Table 2.

The 5 classes of galaxies *outside substructures* were all defined with a fixed upper limit in δ of 1.8 (see Sect. 4.2).

As explained in Sect. 4.2 we defined, for each of the 5 classes of galaxies within substructures, 4 samples with lower limits in δ of 1.8, 2.0, 2.2 and 2.4, respectively. From the results of each set of 4 parallel samples, we gauged the “diluting” effect (by contamination of galaxies with a δ -value above the limit, but not in substructures) on real differences (see also Fig. 2). At the same time, we estimated the influence of the opposite effect, viz. a spurious “difference” due to contamination. In many cases the results of the 4 samples of galaxies in substructures with different lower limits in δ are consistent. There are 12 comparisons which do not show total agreement between the 4 parallel tests. These comparisons are discussed in more detail in Appendix B, where we give the 4 results as well as our interpretation.

With the 10 classes, we did all 45 possible comparisons (which require a total of 150 KS2D tests, due to the 4 lower limits to δ used for the classes of galaxies in substructures). Of these 45 comparisons, 22 show a significant difference. We stress again that the verdict “significant difference” indicates that the probability that the two galaxy samples were drawn from the same parent sample is less than 5%. It should be appreciated that comparisons for which no believable difference was found are “undecided”. In other words: in those cases *it is not proven* that the galaxy samples have identical (R, v) -distributions, because our data do only indicate that they are not significantly different.

The results are as follows:

- Of the 10 comparisons between classes of galaxies *not in substructures*, 6 show a difference: viz. E–S₁, E–ELG, S0–S_e, S0–S₁, S0–ELG and S_e–S₁.
- Of the 10 comparisons between classes of galaxies *in substructures*, 2 show a difference: viz. S0–S₁ and S0–ELG
- Of the 25 “mixed” comparisons between classes of galaxies in and outside substructures, 14 show a difference. The latter are not very surprising in view of the result discussed in Sect. 4.2. Instead, the comparisons for which *no* difference was found may be more informative in this case; these are: E_{sub}–S_{1, nosub}, E_{sub}–ELG_{nosub}, S0_{sub}–S_{e, nosub}, S0_{sub}–S_{1, nosub}, S0_{sub}–ELG_{nosub}, S_{e, sub}–E_{nosub}, S_{e, sub}–S0_{nosub}, S_{e, sub}–S_{e, nosub}, S_{e, sub}–S_{1, nosub}, S_{e, sub}–ELG_{nosub} and S_{1, sub}–S_{1, nosub}.

In view of the sample sizes (see Table 2) the latter 6 results may well be due to limited statistics.

As mentioned in Sect. 2, all projected distances R were expressed in r_{200} , which was derived from the velocity dispersion σ_p on the assumption of a mass profile with $M(< r) \propto r$. We redid all KS2D comparisons with projected distances scaled with an alternative value of r_{200} , calculated for an assumed mass profile $M(< r) \propto \sqrt{r}$. The results are essentially identical, and lead to the same definition of galaxy ensembles, as we describe now.

6.2. The minimum number of galaxy ensembles

Based on the segregation results discussed in Sect. 6.1, we have tried to find the *minimum* number of galaxy samples that *must* be distinguished. The KS2D tests tell us which galaxy classes cannot be combined (i.e. those that have a probability of less than 5% of being drawn from the same parent population), and which classes *can* in principle be combined (those with a probability of more than 5% . . .), but they do not tell us which ones *must* be combined.

We will first consider the classes of galaxies within and outside substructures separately. This is motivated by the fact that the individual galaxy classes, viz. ellipticals, S0s, all spirals (including the generic spirals) and ELG in and outside substructures have different (R, v) -distributions. Note that this is true for all 4 substructure samples (i.e. for different values of δ_{\min}). It is true that our data do not indicate that $S_{e,\text{nosub}}$ and $S_{e,\text{sub}}$ have different (R, v) distributions, and similarly for $S_{l,\text{nosub}}$ and $S_{l,\text{sub}}$, but this may be due to limited statistics.

For the galaxies that are not in substructures, the data do not allow less than three galaxy ensembles. This is because the S_e 's and S_l 's cannot be combined, while at the same time neither of these can be combined with the S0s. According to the other “segregation rules” in Sect. 6.1, the Es and ELG can be combined in three different ways with S0s, S_e 's and S_l 's. E.g., the Es can be combined with S0s as well as S_e 's, while the ELG can be combined with S_e 's and S_l 's, as long as this does not imply combining them with Es or S0s. Two of these three ensemble configurations are not meaningful, because in them there are two ensembles that are not significantly different (i.e., which have more than 5% probability to have been drawn from the same parent population). That leaves a *unique ensemble configuration for the galaxies that are not in substructures*, viz.:

$$- [E_{\text{nosub}}+S0_{\text{nosub}}], S_{e,\text{nosub}}, [S_{l,\text{nosub}}+ELG_{\text{nosub}}].$$

We note in passing that the fact that the Es and S0s outside substructures together constitute an ensemble means that the intermediate galaxy class, $E/S0_{\text{nosub}}$ can be included in that ensemble.

For the galaxies within substructures, the “segregation rules” require a minimum of two ensembles. This is remarkable, because the definition of substructures and the assignment of galaxies to substructures was done totally independent of galaxy type. Applying the “segregation rules” for the galaxies in substructures, we obtain four possible two-ensemble configurations, viz.:

$$\begin{aligned} &- S0_{\text{sub}}, [E_{\text{sub}}+S_{e,\text{sub}}+S_{l,\text{sub}}+ELG_{\text{sub}}] \\ &- [S0_{\text{sub}}+E_{\text{sub}}], [S_{e,\text{sub}}+S_{l,\text{sub}}+ELG_{\text{sub}}] \\ &- [S0_{\text{sub}}+S_{e,\text{sub}}], [E_{\text{sub}}+S_{l,\text{sub}}+ELG_{\text{sub}}] \\ &- [S0_{\text{sub}}+E_{\text{sub}}+S_{e,\text{sub}}], [S_{l,\text{sub}}+ELG_{\text{sub}}]. \end{aligned}$$

In each of these configurations, the two ensembles always have significantly different (R, v) -distributions. Because there is no evidence that we need to separate $S_{e,\text{sub}}$ and

$S_{l,\text{sub}}$, we add the generic spirals (within substructures) to the two ensembles which contain both $S_{e,\text{sub}}$ and $S_{l,\text{sub}}$.

While we were able to identify a unique 3-ensemble configuration for the galaxies outside substructures, our data do not uniquely define the two ensembles into which the galaxies within substructures are segregated. Nevertheless, the 10 galaxy classes that we started with can be reduced to 5 ensembles. However, the choice between the 4 possible 5-ensemble configurations cannot be made with our data.

So far, we have considered ensembles that consist only of galaxies either in or outside substructures. Yet, our data allow combinations of galaxies in and outside substructures in a single ensemble. If such combinations are not considered unacceptable for physical reasons, one can construct ensemble configurations with 4 ensembles instead of 5. The reason is that, even though galaxies of a *given class* have different (R, v) -distributions within and outside substructures (except maybe the S_e and S_l), this is not true in general. In other words: the KS2D tests allow e.g. $S0_{\text{sub}}$ and ELG_{nosub} to be combined. However, no configurations with 3 ensembles are possible. This is because, according to our data, the $[E+S0]_{\text{nosub}}$ cannot be combined with any of the 8 substructure ensembles. The fact that the $[E+S0]_{\text{nosub}}$ can be combined with the $S_{e,\text{sub}}$ which are in one of the two substructure ensembles does not affect that conclusion.

If one tries to construct mixed ensembles, simply by combining the 3 ensembles outside substructures with the 4 sets of 2 ensembles within substructures, one can construct 6 configurations of 4 ensembles. However, there is no good reason why one could then not “open” the 3 ensembles outside substructures and the two within substructures, and the number of possible 4-ensemble configurations then certainly becomes larger than six. However, we do not consider it very useful to explore all those possibilities.

7. The nature of the morphological segregations

Having studied, through KS2D tests in which we compare (R, v) -distributions, which morphological segregations are indicated by our data, it remains to characterize the nature of the various segregations. In Fig. 5 we show the (R, v) -distributions of the following 8 galaxy classes: *outside substructures*, the E_{nosub} with $M < -22$, the $[E+E/S0+S0]_{\text{nosub}}$, the $S_{e,\text{nosub}}$, the $[S_l+ELG]_{\text{nosub}}$, and *in substructures* the E_{sub} , the $S0_{\text{sub}}$, the $S_{e,\text{sub}}$ and the $[S_l+ELG]_{\text{sub}}$. As explained in Sect. 5, the last 7 classes do not contain galaxies with $M < -22$. In order to minimize the effects of contamination in the substructure samples, while still retaining a reasonable statistics, we applied a lower limit in δ of 2.2 (see also Sect. 4.2). Because Es and S0s outside substructures have (R, v) -distributions that are not significantly different, we added the class $E/S0_{\text{nosub}}$ to that sample.

Figure 5 visually illustrates the segregation results discussed in Sects. 5 and 6. The bright ellipticals clearly have

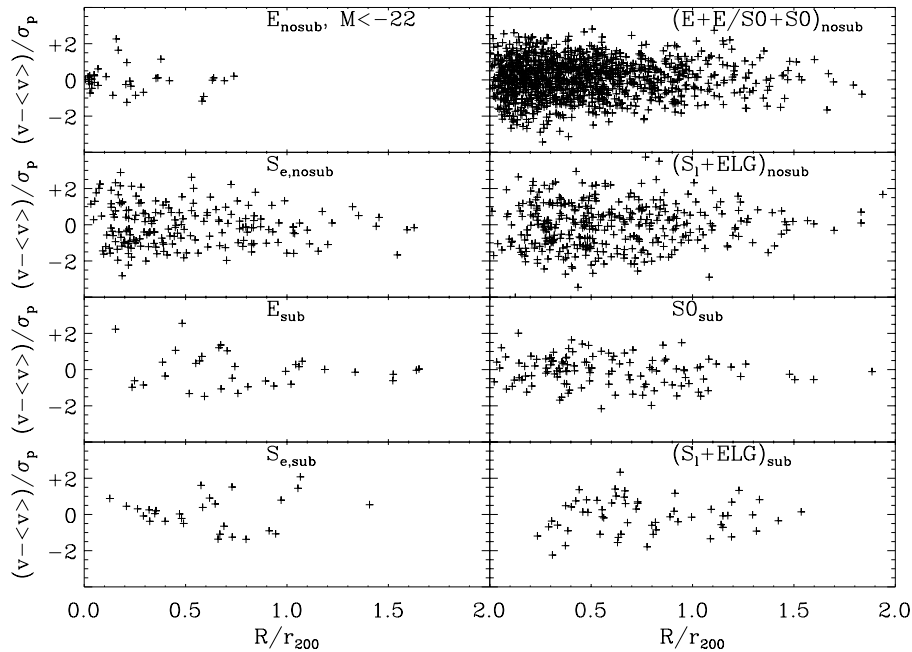


Fig. 5. The (R, v) -distributions of the 8 classes of galaxies implied by the analysis of luminosity and morphology segregation. The samples of galaxies in substructures were defined with a substructure parameter $\delta > 2.2$.

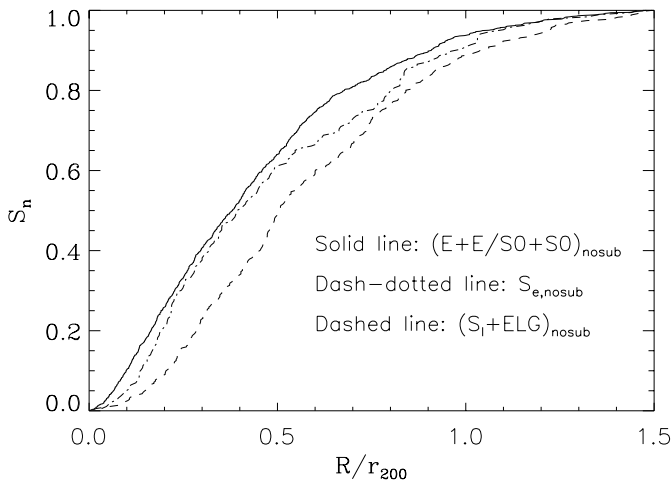


Fig. 6. a) The cumulative R -distribution of the 3 ensembles outside substructures.

a very distinct (R, v) -distribution, unlike that of any of the other classes, and the physical reason for that has been amply discussed in the literature (see, e.g., Governato et al. 2001). Note that the 4 classes of galaxies outside substructures are mutually exclusive, but the 4 classes of galaxies inside substructures are not, and we could combine them into 4 possible configurations of 2 ensembles (see Sect. 6.2). However, we do not show the (R, v) -distributions of all these possible configurations here.

7.1. The ensembles of galaxies outside substructures

The 3 ensembles of galaxies that are not in substructures, viz. $[E+E/S0+S0]_{\text{nosub}}$, $S_{e,\text{nosub}}$ and $[S_1+ELG]_{\text{nosub}}$ are indeed seen to have different (R, v) -distributions. The na-

ture of these differences is illustrated in the form of cumulative distributions of R and v in Fig. 6. Figure 6a shows clearly that the $[E+E/S0+S0]_{\text{nosub}}$ (the early-type galaxies) are the most centrally concentrated of the 3 ensembles. For $R/r_{200} \lesssim 0.5$, the shape of the distribution of the $S_{e,\text{nosub}}$ is quite similar to that of the early-type galaxies, but at larger distances it may become slightly wider. The distribution of the $[S_1+ELG]_{\text{nosub}}$ (the late-type galaxies) is widest of all, and flattens strongly towards the centre.

Because the velocity distributions depend on R/r_{200} , we show, in Fig. 6b, the cumulative velocity distributions for three radial intervals. In the inner region ($R/r_{200} < 0.25$) the $S_{e,\text{nosub}}$ and the late-type galaxies have very similar velocity distributions, which are significantly broader than that of the early-type galaxies. Instead, in the intermediate radial interval ($0.25 \leq R/r_{200} < 0.75$), the velocity distributions of the $S_{e,\text{nosub}}$ and early-type galaxies are very similar, while that of the late-type galaxies is broader than the other two. Finally, for $0.75 \leq R/r_{200} \leq 1.5$ the three distributions are quite similar, although there is a weak hint that now the velocity distribution of the $S_{e,\text{nosub}}$ galaxies may be even narrower than that of the other ensembles. Although the differences between early- and late-type galaxies are not completely new, they are now demonstrated with unprecedented statistical weight and detail.

However, the behaviour of the $S_{e,\text{nosub}}$ galaxies was not seen before and is very intriguing. The segregation of $S_{e,\text{nosub}}$ and $S_{1,\text{nosub}}$, although significant with our adopted probability limit of 5%, is not the strongest segregation that we find. Therefore, it is gratifying to see that there is also a good physical reason for distinguishing the $S_{e,\text{nosub}}$ as a separate class, namely the fact that their

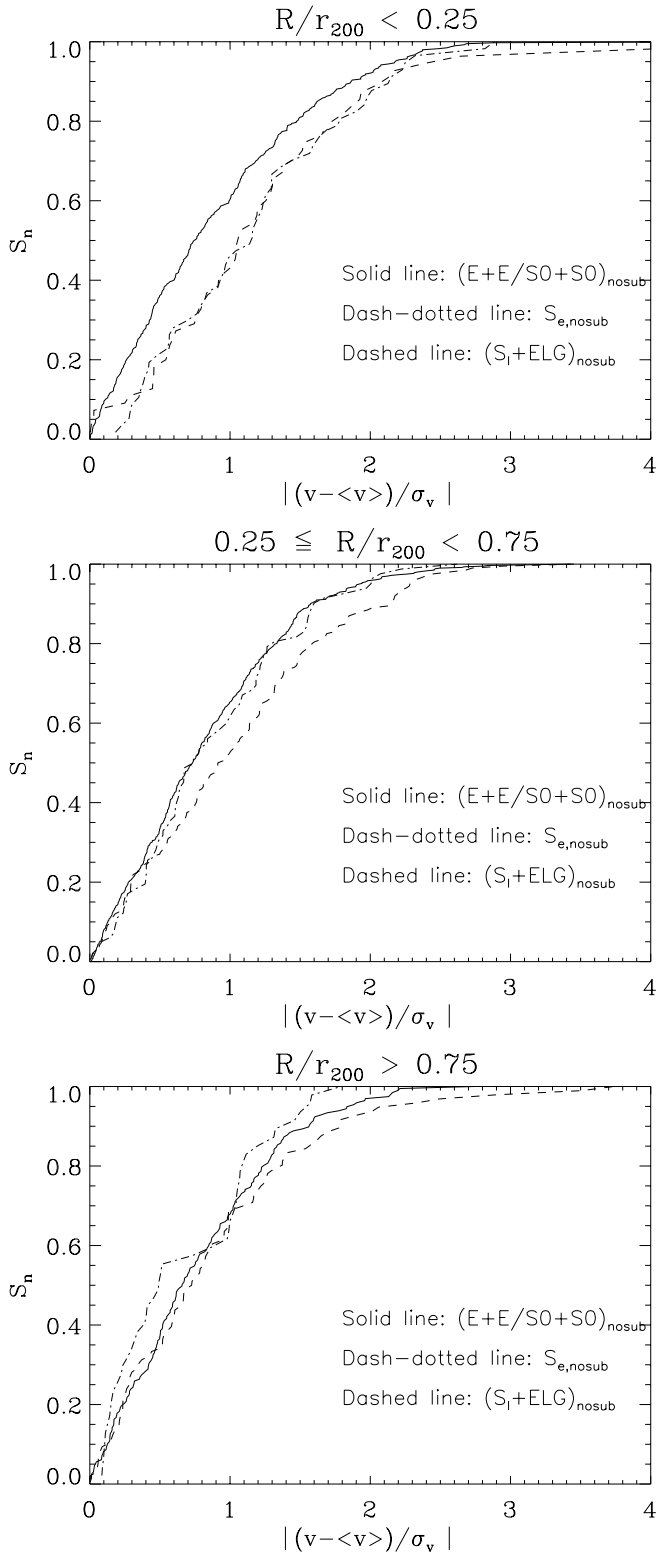


Fig. 6. b) The cumulative v -distributions of the 3 ensembles outside substructures, in three different radial ranges.

velocity distribution changes “allegiance” from inside to outside. Further support for the reality of and need for a separate $S_{e,nosub}$ class comes from the KS2D comparisons of the $S_{e,nosub}$ with the $[E+E/S0+S0]_{nosub}$ and the

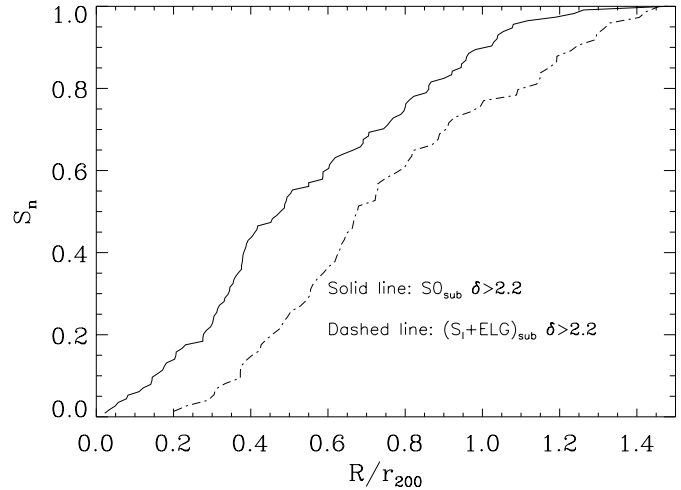


Fig. 7. a) The cumulative R -distributions of S0 and $[S_l+ELG]$ galaxies in substructures.

$[S_l+ELG]_{nosub}$, both of which show the three ensembles to be different.

7.2. The ensembles of galaxies in substructures

The segregation of the classes of galaxies in substructures is much less clean-cut than it is for those outside substructures. In itself, it is remarkable that the galaxies inside substructures should show segregation at all, because the selection of galaxies with $\delta > \delta_{lim}$ (with $\delta_{lim} = 1.8, 2.0, 2.2$ and 2.4) was made independent of galaxy type. Yet, the KS2D tests indicate that the S0s in substructures have an (R, v) -distribution that is different from both S_l 's and ELG separately, as well as from $[S_l+ELG]$. The (R, v) -distributions of $S0_{sub}$ and $[S_l+ELG]_{sub}$ in Fig. 5 (where $\delta_{lim} = 2.2$) provide visual support for the difference.

As we did for the ensembles outside substructures, we illustrate the nature of the segregation between $S0_{sub}$ and $[S_l+ELG]_{sub}$ with cumulative distributions of projected distance and relative velocity. In Fig. 7a we show the cumulative radial distributions for $\delta_{lim} = 2.2$. The difference between the two radial distributions is quite clear. Yet, contamination by S0s outside substructures could be partly responsible for the difference. However, the difference in Fig. 7b indicates that the late-type galaxies in substructures not only have a shallower radial distribution but also a larger velocity width than the S0s. This latter fact cannot be attributed to contamination by S0s outside substructures, particularly because the latter have (if anything) a larger velocity width than the S0s inside substructures.

8. Discussion

8.1. Summary of our findings

We start the discussion of the implications of our analysis by summarizing the main results and by putting these in a broader perspective.

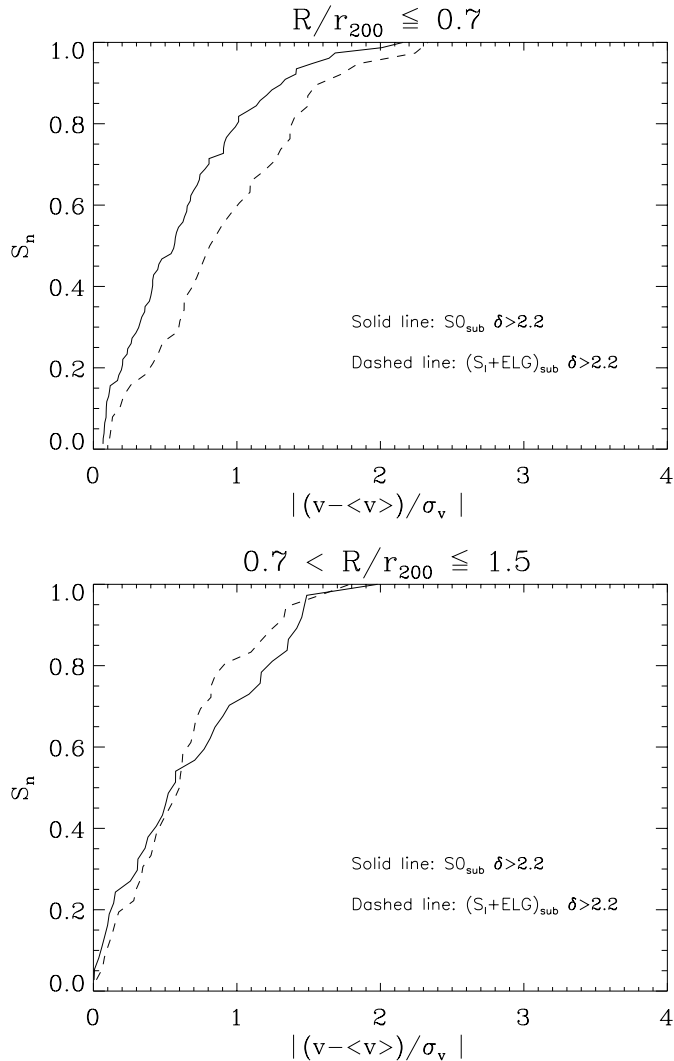


Fig. 7. b) The cumulative v -distributions of S0 and [S₁+ELG] galaxies in substructures, in two different radial ranges.

Our *first conclusion* concerns *luminosity segregation*. We only find significant luminosity segregation for the brightest Es outside substructures. Had the S0s outside substructures shared the luminosity segregation of the Es, the statistical weight of our data would have been more than sufficient to detect it. Thus, our result is more in line with that by Stein (1997) than with that by Biviano et al. (1992). The absolute magnitude M_R of -22 which separates the brightest Es (those that show LS) from the other Es agrees nicely with that found by Biviano et al. (1992) as the limit for kinematical segregation (using $V - R \simeq 0.6$ for early-type galaxies, see, e.g., Poulain & Nieto 1994). Of the 42 Es in our sample with $M_R < -22$, about two-thirds are first-ranked galaxies. The brightest Es, which mostly occur outside substructures, thus appear to form a really separate population which is very centrally concentrated and kinematically quite cold, and which probably mostly has an accretion and merger origin (see, e.g., Governato et al. 2001).

Global estimates of the timescale for dynamical friction in an average ENACS cluster yields about 1 Gyr for

the brightest ellipticals and for the 1st-ranked galaxies, and about 2 Gyr for the 2nd-ranked galaxies. So, dynamical friction can be very well responsible for the luminosity segregation that we observe. Given these estimates it is perhaps somewhat surprising that the 2nd-ranked galaxies do not show evidence for luminosity segregation. This could indicate that the 2nd-ranked galaxies are being cannibalized by the 1st-ranked galaxies when they get too close to the cluster centre.

The *second conclusion* concerns *substructure*. For Es, S0s, spirals as well as ELG, the (R, v) -distributions of galaxies in and outside substructures are significantly different. This mostly reflects the fact that galaxies in and outside substructures have very different radial distributions (see Fig. 5). In particular, the small fraction of galaxies in substructures within $R \approx 0.3 r_{200}$ probably supplies most of the “signal” for the differences detected by the KS2D tests. As we argued in Sect. 4.3, this effect is most likely real and not induced by the radial dependence of the “size” of groups in our selection of galaxies in substructures.

The *third conclusion* concerns the *galaxies outside substructures*. We find that we must distinguish 4 different classes, viz: 1) the brightest Es, 2) all but the brightest Es combined with the S0s, 3) the S_{late} combined with the ELG and 4) the S_{early}. Thus, excluding the brightest Es, the projected distribution and kinematics of the Es and the S0s are not significantly different. This would follow naturally if these two classes had a common origin and evolution, or if they formed one class. The latter was suggested by Jørgensen & Franx (1994), who concluded that the Es and S0s form one class with a continuous change in $L_{\text{disk}}/L_{\text{total}}$, with the different classifications mostly induced by the viewing angle. It is true that structural differences between Es and S0s now appear much smaller than was once thought, while the stellar populations are also very similar. However, Thomas et al. (2002) conclude, from 194 Es and 307 S0s in 42 ENACS clusters, that viewing angle plays an important rôle, but is probably not the only factor that determines the outcome of the classification. It is also not clear that the morphology-density relation, and its reported dependence on redshift (e.g. Dressler et al. 1997) is consistent with the picture of Jørgensen & Franx (1994).

The late spirals and ELG cannot be distinguished either from their distributions in the (R, v) -plane. This is not very surprising as a large fraction of the ELG (which are all late-type galaxies as the few ELG associated with early-type galaxies were excluded) is associated with *late* spirals. However, the process responsible for the removal of the gas that gives rise to the emission lines apparently does not create any differences between the spatial distribution and kinematics of the late spirals without gas and those with gas (i.e. the ELG). As a matter of fact, our result confirms the general assumption that the gas-removal process changes only the appearance of the galaxy but not its velocity. In other words: we should have been

very surprised if the observations had shown differences in (R, v) -distributions as a result of the gas-removal process.

Finally, the early spirals appear to be a separate class among the galaxies outside substructures. This is quite a robust result: the (R, v) -distributions of the 183 S_e 's and the 1160 E+E/S0+S0s have a 4.1% probability to have been drawn from the same parent distribution, and for the 183 S_e 's and the 349 $[S_1+ELG]$ this is 2.0%. This result is also new and it may have important consequences for the picture of the evolution and transformation of galaxies in clusters. Most intriguing is the fact that the velocity distribution of the S_e 's is very similar to that of the $[S_1+ELG]$ in the very centre, while it is closer to that of the Es+S0s beyond $\sim 0.3 r_{200}$.

The *fourth conclusion* concerns the *galaxies in substructures*. There are two comparisons that show a significant difference, viz. S0 vs. S_1 and S0 vs. ELG, and since we are allowed to combine S_1 and ELG, we checked that S0 and S_1+ELG are also significantly different. It thus appears that the total fraction of galaxies in substructures decreases strongly within $R \sim 0.3 r_{200}$, but that the fraction of S0s in substructures increases within $R \sim 0.3 r_{200}$.

We now turn to a more qualitative discussion of the implications of our results for current ideas about formation, evolution and transformation of galaxies in clusters.

8.2. Galaxies in substructures

The properties of substructures contain a clear clue about the evolution of the clusters as a whole, and of the galaxies within them. The fraction of galaxies in substructures, which on average is about 0.22 (not to be confused with the canonical value of one-third for the fraction of clusters with significant substructure, e.g. Geller & Beers 1982; Dressler & Schectman 1988; Jones & Forman 1992) is correlated with the amount of central concentration of the total galaxy population. While the central concentration increases with time, the fraction of galaxies in substructures decreases. In other words: substructures are destroyed in the course of time, probably mostly through tidal stripping in the central regions, on time-scales that are fairly short. The longest survival times are for high-density groups on non-radial orbits (e.g., González-Casado et al. 1994).

In this picture, the strong decrease of the fraction of galaxies in substructures for $R \lesssim 0.3 r_{200}$ is not surprising. However, the new and unexpected result is that the composition of the substructures changes towards the centre, and in particular within $R \sim 0.3 r_{200}$. Most noticeably, the fraction of S0s in substructures increases strongly towards the centre. This is evident from inspection of Fig. 5; however, in view of the R -distribution of the S0s outside substructures, one wonders how much of this effect could be due to contamination by a small fraction of S0s outside substructures (the largest galaxy class in our clusters).

In Fig. 8 we show the composition of substructures as a function of R/r_{200} . The relative contributions of the

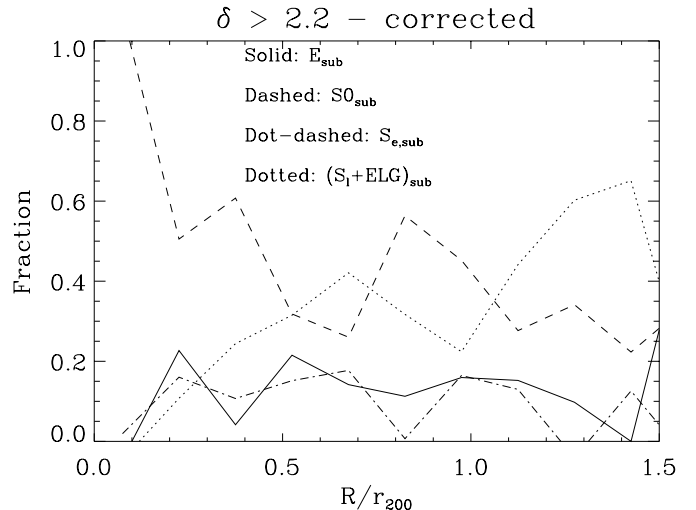


Fig. 8. The composition of substructures as a function of projected radius R .

4 classes have been corrected for accidental substructure. This was done by subtracting from the observed numbers the average number of galaxies of each type found in 100 azimuthal resamplings of the data. I.e., whatever contamination is still present in Fig. 5 has been taken out in Fig. 8. The latter figure thus confirms the reality of the increase of the fraction of S0s, which is accompanied by a decrease of the fraction of S_1+ELG towards the centre in substructures. In other words: it appears that in the substructures that survive in the central regions, the $[S_1+ELG]$ have a harder time to survive than the S0s. On the basis of the evidence in Fig. 8 it thus seems that the late spirals in subclumps are not protected very well against stripping and “conversion”. The fractions of Es and S_e 's in substructures do not show a dependence on distance, but this may partly be due to limited statistics.

As a matter of fact, the fraction of $[S_1+ELG]$ in substructures within $R/r_{200} < 0.3$ ($= 0.04 \pm 0.02$) is even smaller than that of the S_1+ELG outside substructure within $R/r_{200} < 0.3$ (0.19 ± 0.04), at the 3.8σ -level. This probably implies that, even within subclumps, late spirals suffer stripping through ram-pressure and turbulence or viscosity that is similar to the general stripping held responsible for the transformation of spirals into S0s (e.g. Abadi et al. 1999; Quilis & Moore 2001). Actually, the data seem to imply that the tidal stripping of the subclumps, when they approach the centre, makes life even harder for the late spirals in substructures than for the late spirals outside substructures. However, the processes by which the life of late spirals becomes harder when the subclumps in which they find themselves approach the centre are not at all clear, as transformation within subclumps of late spirals into S0s does not seem very likely.

8.3. Galaxies outside substructures

For the galaxies outside substructures (remember, this is the large majority), the situation is different. This

population contains a contribution of galaxies (especially in the central region) that entered the cluster as members of subclumps. However, it is likely that most of the galaxies outside substructures entered the cluster from the field, mostly as late-type galaxies, and partly as Es that formed in small groups prior to entry into the cluster (Pence 1976; Dressler 1980; Merritt 1985). This infall picture is also supported by evidence on the radial anisotropy of the orbits of the late-type galaxies (as seen e.g. in the ENACS cluster sample, see Papers III and VI).

Spurred by the seminal results of Butcher & Oemler (1984) and Dressler et al. (1997) there have, in recent years, been many investigations, both observational and theoretical, of the influence of the cluster environment on the galaxies. The morphological composition of clusters is observed to change with redshift, and the usual interpretation is that S0s have formed relatively recently through transformation of spirals (Dressler et al. 1997; Fasano et al. 2000). The details of the transformation were studied in several ways. Poggianti et al. (1999) discuss spectral evidence for a two-stage transformation, while Jones et al. (2000) conclude that the most likely progenitors of S0s in rich clusters are early spirals in which starformation was quenched.

The mechanisms by which galaxies in clusters may evolve and transform have been modelled by several groups, e.g. Moore et al. (1998, 1999), Abadi et al. (1999), Diaferio et al. (2000), and Okamoto & Nagashima (2001). The processes that can affect the morphologies of discs are e.g. stripping of gas through ram-pressure (Gunn & Gott 1972; Abadi et al. 1999) or turbulence and viscosity (Quilis et al. 2001), impulsive tidal interactions between galaxies (Moore et al. 1998, 1999), and mergers (e.g. Barnes & Hernquist 1996). Comparison of the results of such models with observations is not trivial, because model parameters must be translated into observables. E.g., deriving the morphological type from a bulge-to-disk ratio alone may not be subtle enough, and that could be one of the reasons why Okamoto & Nagashima (2001) fail to reproduce the well-established morphology-density relation.

From numerical models, Moore et al. (1999) found that the fate of spiral galaxies in clusters depends very much on the amount of central concentration of the distribution of total mass. Spirals with slowly rising rotation curves (i.e. not centrally concentrated) have between 50 and 90% of their stars stripped after 10 Gyrs or so, through impulsive interactions with other galaxies. On the contrary, the galaxies with more centrally concentrated mass distributions can survive relatively unscathed, albeit that the scale height of their stellar disc in general increases through tidal heating.

In the context of our segregation results, it is quite relevant that there is a significant correlation between the morphology of a spiral galaxy and the form of its rotation-curve (see e.g. Corradi & Capaccioli 1990; Biviano et al. 1991; Adami et al. 1999; Dale et al. 2001). Flat rotation curves (which indicate a centrally peaked mass distribution) are seen much more often for early spirals than for

late spirals, for which the rotation curves are more often rising (indicating a less centrally peaked mass distribution). The relative paucity of late spirals in the central region probably indicates that most late spirals in the centre have been destroyed. On the other hand, the early spirals can survive in the centre, and the different radial distributions of early and late spirals probably just reflect the different shapes of their potential wells.

As shown in Paper VIII, the fraction of ELG among early spirals is significantly lower than the fraction of ELG among late spirals (0.19 ± 0.03 and 0.56 ± 0.05 , respectively, for the sample considered in the present paper). Part of this difference could be intrinsic (Gavazzi et al. 1988), but there may also be a contribution from the difference in the radial distribution. In any case, the result is similar to the radial dependence of the HI deficiency as discussed by Solanes et al. (2001). Actually, within 1.0 Abell radius ($\sim 1.25 r_{200}$) the HI deficiency is systematically higher for the early spirals than it is for the late spirals. Solanes et al. (2001) interpret this as evidence for the fact that early spirals are more easily emptied of their gas. The difference in radial distribution could also be a factor, although Thomas (2002) finds no evidence for that.

Finally, we turn to the relation between the early spirals and the S0s. While their (R, v) -distributions are different according to the KS2D comparison, closer inspection reveals that most of the signal for that difference is in relative velocity. Actually, the radial distribution of the early spirals is indistinguishable from that of the S0s. This may or may not be good news, depending on one's prejudices about the radial variation of the efficiency with which impulsive encounters transform early spirals into S0s. Yet, the data seem to indicate an almost constant efficiency of the transformation of early spirals into S0s. If this is indeed the case, the density increase towards the centre apparently is largely offset by the larger velocities. In this picture, the difference in line-of-sight velocity dispersion of the early spirals and S0s, within $\sim 0.3 r_{200}$, must have a natural explanation. E.g., it could be that the early spirals that have survived have obtained a velocity distribution that makes them relatively unsusceptible to transformation into an S0.

9. Summary and conclusions

We have studied evidence for luminosity and morphology segregation in an ensemble cluster of ~ 3000 galaxies with positions, magnitudes, velocities, and galaxy types, in clusters observed in the ESO Nearby Abell Cluster Survey. From positions and velocities we identify galaxies in and outside substructures. The fraction of galaxies in substructures appears to decrease strongly towards the cluster centre. Luminosity segregation is evident only for the very bright ($M_R \lesssim -22$) ellipticals outside substructures, which mostly are brightest cluster members near the centres of their clusters.

For galaxies of all types, we find that those within substructures are segregated with respect to those outside

Table A.1. The 59 ENACS clusters with at least 20 member galaxies, and galaxy types for at least 80% of the members.

ACO	α_{centre} 1950.0	δ_{centre}	\bar{v}_{3K}	σ_p	N_z	N_m	N_t	ACO	α_{centre} 1950.0	δ_{centre}	\bar{v}_{3K}	σ_p	N_z	N_m	N_t
13	00 11 00	-19 46.7	27949	897	37	37	37	3094	03 09 48	-27 09.9	20027	654	66	66	64
87	00 40 13	-10 04.3	16149	875	27	27	27	3111	03 15 55	-45 51.8	23179	770	35	35	34
119	00 53 40	-01 30.3	12997	720	104	102	87	3112	03 16 12	-44 25.2	22417	954	76	67	60
151	01 06 27	-16 12.7	12074	403	25	25	25	3122	03 20 21	-41 31.4	19171	782	90	89	88
151	01 06 24	-15 41.2	15679	747	46	44	44	3128	03 28 50	-52 42.9	17931	765	155	152	152
151	01 06 08	-15 53.3	29459	804	34	33	33	3151	03 38 21	-28 50.2	20352	752	34	34	34
168	01 12 35	00 05.4	13201	518	76	76	71	3158	03 41 25	-53 47.9	17698	1006	105	105	102
295	01 59 44	-01 22.1	12490	298	30	30	26	3194	03 57 10	-30 18.7	29111	797	32	32	32
514	04 46 11	-20 34.4	21374	875	90	82	74	3202	03 59 24	-53 49.3	20741	435	27	27	27
524	04 55 40	-19 47.0	23262	802	26	26	25	3223	04 06 34	-30 57.2	17970	597	68	66	65
548	05 46 39	-25 27.8	12400	710	111	108	108	3341	05 23 43	-31 38.6	11364	561	63	63	63
548	05 43 26	-25 55.5	12638	824	125	120	116	3354	05 33 04	-28 34.2	17589	367	58	56	56
754	09 06 35	-09 27.1	16754	1010	38	38	38	3365	05 46 14	-21 56.5	27879	1151	32	32	32
957	10 11 17	-00 39.3	13661	649	34	32	31	3528	12 51 40	-28 44.4	16377	971	28	28	28
978	10 17 56	-06 16.5	16648	497	58	56	52	3558	13 25 09	-31 13.7	14571	1035	75	73	73
1069	10 37 18	-08 24.8	19909	937	32	32	31	3559	13 27 04	-29 15.4	14313	425	39	38	37
1809	13 50 35	05 24.2	24169	774	30	30	30	3562	13 31 01	-31 25.3	14633	903	111	105	105
2040	15 10 21	07 36.7	13974	675	37	37	37	3651	19 48 10	-55 11.4	17863	662	79	78	78
2048	15 12 50	04 34.1	29303	661	25	25	25	3667	20 08 24	-56 57.8	16620	1037	103	103	102
2052	15 14 15	07 11.1	10638	719	33	33	27	3691	20 30 55	-38 12.7	26021	699	31	31	31
2361	21 36 08	-14 32.3	17924	332	24	24	24	3705	20 38 54	-35 23.9	26687	1059	29	29	29
2401	21 55 36	-20 20.6	16844	475	23	23	22	3764	21 22 48	-34 56.9	22442	583	36	36	34
2569	23 14 54	-13 05.7	23897	482	36	36	36	3806	21 42 55	-57 31.0	22825	808	97	84	83
2734	00 08 47	-29 08.1	18217	579	83	77	77	3822	21 50 40	-58 06.2	22606	871	84	84	68
2799	00 35 02	-39 24.3	18724	423	36	36	36	3825	21 54 44	-60 41.5	22373	699	59	59	57
2800	00 35 29	-25 20.9	18777	400	33	33	27	3827	21 58 26	-60 10.8	29338	1132	20	20	20
2819	00 43 46	-63 49.0	22285	409	49	49	44	3879	22 24 05	-69 16.7	19982	444	42	42	36
2819	00 43 54	-63 52.2	25864	353	43	43	41	3921	22 46 43	-64 41.7	27907	495	31	30	30
2911	01 23 51	-38 13.5	24012	404	29	27	27	4010	23 28 34	-36 46.7	28437	622	30	30	30
3093	03 09 15	-47 35.1	24771	408	22	21	20								

substructures. This is mostly due to the fact that galaxies in and outside substructures have very different radial distributions. In addition, morphology segregation is found among galaxies both *in* and *outside* substructures.

The early- and late-type galaxies *outside substructures* have different (R, v) -distributions, i.e. of projected position R and relative velocity v . The early-type galaxies except the brightest ellipticals all have very similar (R, v) -distributions, i.e. the fainter ellipticals and S0s are not segregated. Similarly, the late spirals and the emission-line galaxies have indistinguishable (R, v) -distributions, but the (R, v) -distribution of the early spirals differs from that of the early-type galaxies and from that of the other late-type galaxies. Among galaxies *in substructures*, the S0s are segregated from the late spirals and the emission-line galaxies, both separately as well as taken together.

Luminosity segregation is most likely due to the dissipative processes in the innermost region of the clusters, which presumably produce the brightest ellipticals. The decrease of the fraction of galaxies in substructures towards the centre is probably due to tidal disruption. The cause for the accompanying decrease of the fraction of late-type galaxies in the subclumps is not evident, in particular because the latter is even stronger than the decrease

towards the centre of the fraction of late-type galaxies outside substructures.

The large difference between the radial distributions of early and late spirals are attributed to systematic differences in their mass profiles. The late spirals presumably are fairly easily destroyed through impulsive encounters with other galaxies, and the early spirals much less, so that they can survive in the inner cluster regions. We briefly discuss the constraints that our data provide for the process by which early spirals transform into S0s.

Acknowledgements. AB and PK acknowledge the hospitality of Leiden Observatory and Trieste Observatory, respectively. This research was partly supported by the *Consorzio Nazionale per lo studio della Formazione ed evoluzione delle galassie* and by the Leids Kerkhoven-Bosscha Fonds. We thank Tim de Zeeuw for a careful reading of the manuscript.

Appendix A: The clusters used in the analysis

Details about the 59 clusters used in the analysis are given in Table A.1, which contains the following information:

Column 1: The ACO number of the system.

Columns 2 and 3: The adopted position of the cluster centre.

Column 4: Average velocity of the system in the CMBR

reference frame (km s^{-1}).

Column 5: The overall velocity dispersion computed from all cluster members (km s^{-1}).

Column 6: Total number of galaxies with redshifts, N_z .

Column 7: Number of member galaxies with ENACS redshifts, N_m .

Column 8: Number of member galaxies with ENACS redshifts and galaxy type, N_t .

Note that the two systems in A548 with essentially the same redshift are spatially distinct; the one at 12278 km s^{-1} is the eastern component of this double cluster, that at 12736 km s^{-1} is the western component. For 17 clusters we had no CCD-imaging (ACO nrs. 524, 1809, 2048, 2819 ($\bar{v} = 22285$), 2819 ($\bar{v} = 25864$), 3151, 3158, 3194, 3202, 3365, 3651, 3691, 3705, 3822, 3827, 3921 and 4010), and in 6 clusters (ACO Nos. 2799, 3112, 3122, 3559, 3825 and 3827) the fraction of galaxy types from CCD-imaging is less than 50%.

Appendix B: KS2D tests with ambiguous results, involving galaxies in substructures

Here we give details about the 12 KS2D comparisons which involve at least one sample of galaxies inside substructures, and which do not give identical results at all 4 values of δ_{lim} (see Sect. 6.1). In Table B.1 the results of each of these 4 comparisons are given, where an “X” indicates that the probability that the two samples are drawn from the same parent sample is less than 5%. We have interpreted the results as follows.

In general, there are two effects that can mask a real difference: limited statistics, and contamination by galaxies outside substructures in a sample of galaxies within substructures. Imagine a comparison between a sample of galaxies outside substructures and a sample of galaxies in substructures. The former will hardly be contaminated by galaxies in substructures, but the latter will inevitably contain some galaxies outside substructures. These contaminating galaxies may mask a real difference, namely when their distribution is similar to that of the galaxies in the other sample. On the other hand, contamination can also induce a spurious difference between two samples. If the galaxies outside substructures, which contaminate the substructure sample, are distributed differently from the galaxies in the other sample, they may create a spurious difference. Contamination is more important at low δ_{lim} , but if we use a higher δ_{lim} , to reduce contamination, we pay in terms of limited statistics.

For the comparisons in Table B.1 we now summarize the reason for our adopted result. In the comparison $S0_{\text{sub}}$ vs. ELG_{nosub} limited statistics is assumed to be cause for the result at the highest value of δ_{lim} . Limited statistics is also held responsible for absence of a difference in two of the four comparisons between $S_{1,\text{nosub}}$ and ELG_{sub} . In this case, the difference at $\delta_{\text{lim}} = 1.8$ is taken to be real, because the contaminants in the ELG_{sub} sample can only reduce the significance of the difference (since

Table B.1. Tests with ambiguous results involving substructure samples.

samples	δ_{lim}				adopted
	1.8	2.0	2.2	2.4	
$S0_{\text{sub}} - ELG_{\text{sub}}$	X	X	X		different
$S_{1,\text{nosub}} - ELG_{\text{sub}}$	X			X	different
$E_{\text{nosub}} - E_{\text{sub}}$		X	X	X	different
$E_{\text{sub}} - S0_{\text{nosub}}$		X	X	X	different
$S_{e,\text{nosub}} - S_{1,\text{sub}}$		X	X	X	different
$S_{e,\text{nosub}} - E_{\text{sub}}$			X	X	different
$E_{\text{sub}} - ELG_{\text{sub}}$	X				not different
$ELG_{\text{nosub}} - S0_{\text{sub}}$	X				not different
$S_{1,\text{nosub}} - S0_{\text{sub}}$	X				not different
$S_{1,\text{sub}} - ELG_{\text{nosub}}$			X		different
$S_{1,\text{sub}} - S0_{\text{sub}}$		X			different
$S_{e,\text{nosub}} - S0_{\text{sub}}$		X			not different

$S_{1,\text{nosub}}$ and ELG_{nosub} share the same distribution). The same explanation probably applies to the next four comparisons: (E_{nosub} vs. E_{sub} , E_{sub} vs. $S0_{\text{nosub}}$, $S_{e,\text{nosub}}$ vs. $S_{1,\text{sub}}$, $S_{e,\text{nosub}}$ vs. E_{sub}). The contaminants in the “substructure” samples probably mask a real difference when δ_{lim} is set too low. The opposite effect is considered to determine the results for the comparisons E_{sub} vs. ELG_{sub} , ELG_{nosub} vs. $S0_{\text{sub}}$, and $S_{1,\text{nosub}}$ vs. $S0_{\text{sub}}$, which show a significant difference only at the lowest δ_{lim} . Yet, in these cases, contamination of non-substructure galaxies into the substructure samples is likely to be responsible for the difference.

The interpretation of the last three comparisons is less clear. In the $S_{1,\text{sub}}$ vs. ELG_{nosub} comparison, the sample of $S_{1,\text{sub}}$ is very small, and we certainly run into problems of limited statistics at high δ_{lim} values. On the other hand, at low δ_{lim} , a significant contamination of S_1 outside substructures can make the distribution of the $S_{1,\text{sub}}$ sample resemble that of ELG_{nosub} . Therefore, we conclude that these samples are probably different. The four comparisons between $S_{1,\text{sub}}$ and $S0_{\text{sub}}$ give only one significantly different result. However, given the small number of $S_{1,\text{sub}}$, this is remarkable. We therefore think we can trust this result, and ascribe the other negative results to a problem of limited statistics. In the last comparison, statistics are much less of a problem, and we should expect the result at $\delta_{\text{lim}} = 2.0$ to be confirmed at higher values of δ_{lim} . As this is not the case, we conclude that $S_{e,\text{nosub}}$ and $S0_{\text{sub}}$ are not different.

References

- Abadi, M. G., Moore, B., & Bower, R. G. 1999, MNRAS, 308, 947
- Adami, C., Biviano, A., & Mazure, A. 1998a, A&A, 331, 439
- Adami, C., Mazure, A., Biviano, A., Katgert, P., & Rhee, G. 1998b, A&A, 331, 493
- Adami, C., Mazure, A., Katgert, P., & Biviano, A. 1998c, A&A, 336, 63, Paper VII
- Adami, C., Marcelin, M., Amram, P., & Russeil, D. 1999, A&A, 349, 812

- Andreon, S. 1994, *A&A*, 284, 801
 Andreon, S. 1996, *A&A*, 314, 763
 Andreon, S. 1998, *ApJ*, 501, 533
 Barnes, J. E., & Hernquist, L. 1996, *ApJ*, 471, 115
 Beers, T. C., Flynn, K., & Gebhardt, K. 1990, *AJ*, 100, 32
 Bird, C. M. 1994, *AJ*, 107, 1637, 311, 95
 Biviano, A., Girardi, M., Giuricin, G., Mardirossian, F., & Mezzetti, M. 1991, *ApJ*, 376, 458
 Biviano, A., Girardi, M., Giuricin, G., Mardirossian, F., & Mezzetti, M. 1992, *ApJ*, 396, 35
 Biviano, A., Katgert, P., Mazure, A., et al. 1997, *A&A*, 321, 84, Paper III
 Burstein, D., & Heiles, C. 1982, *AJ*, 87, 1165
 Butcher, H., & Oemler, A. Jr. 1984, *ApJ*, 285, 426
 Caon, N., & Einasto, M. 1995, *MNRAS*, 273, 913
 Capelato, H. V., Gerbal, D., Mathez, G., et al. 1980, *ApJ*, 241, 521
 Carlberg, R. G., Yee, H. K., & Ellingson, E. 1997a, *ApJ*, 478, 462
 Carlberg, R. G., Yee, H. K. C., Ellingson, E., et al. 1997b, *ApJ*, 476, L7
 Colless, M., & Dunn, A. M. 1996, *ApJ*, 458, 435
 Corradi, R. L. M., & Capaccioli, M. 1990, *A&A*, 237, 36
 Couch, W. J., Barger, A. J., Smail, I., Ellis, R. S., & Sharples, R. M. 1998, *ApJ*, 497, 188
 Dale, D. A., Giovanelli, R., Haynes, M. P., Hardy, E., & Campusano, L. E. 2001, *AJ*, 121, 1886
 den Hartog, R. 1997, *MNRAS*, 284, 286
 den Hartog, R., & Katgert, P. 1996, *MNRAS*, 279, 349
 de Theije, P. A. M., & Katgert, P. 1999, *A&A*, 341, 371, Paper VI
 Diaferio, A., Kauffmann, G., Balogh, M. L., et al. 2000, *MNRAS*, 323, 999
 Dressler, A. 1980, *ApJ*, 236, 351
 Dressler, A., & Schectman, S. A. 1988, *AJ*, 95, 985
 Dressler, A., Oemler, A., Couch, W., et al. 1997, *ApJ*, 490, 577
 Evrard, A. E., Silk, J., & Szalay, A. S. 1990, *ApJ*, 365, 13
 Fasano, G., & Franceschini, A. 1987, *MNRAS*, 225, 155
 Fasano, G., Poggianti, B. M., Couch, W. J., et al. 2000, *ApJ*, 542, 673
 Fusco-Femiano, R., & Menci, N. 1998, *ApJ*, 498, 95
 Gavazzi, G., Catinella, B., Carrasco, L., Boselli, A., & Contursi, A. 1998, *AJ*, 115, 1745, *AJ*, 107, 2067
 Geller, M. J., & Beers, T. C. 1982, *PASP*, 94, 421
 Giovanelli, R., Haynes, M. P., & Chincarini, G. L. 1986, *ApJ*, 300, 77
 Giuricin, G., Mardirossian, F., Mezzetti, M., Pisani, A., & Ramella, M. 1988, *A&A*, 192, 95
 González-Casado, G., Mamon, G. A., & Salvador-Solé, E. 1994, *ApJ*, 433, L61
 Governato, F., Ghigna, S., Moore, B., et al. 2001, *ApJ*, 547, 555
 Gunn, J. E., & Gott, J. R. 1972, *ApJ*, 176, 1
 Jones, C., & Forman, W. 1992, *Clusters and Superclusters of Galaxies*, ed. A. C. Fabian (Kluwer), 49
 Jones, L., Smail, I., & Couch, W. J. 2000, *ApJ*, 528, 118
 Jørgensen, I., & Franx, M. 1994, *ApJ*, 433, 553
 Kashikawa, N., Sekiguchi, M., Doi, M., et al. 1998, *ApJ*, 500, 750
 Katgert, P., Mazure, A., Perea, J., et al. 1996, *A&A*, 310, 8, Paper I
 Katgert, P., Mazure, A., den Hartog, R., et al. 1998, *A&AS*, 129, 399, Paper V
 Katgert, P., et al. 2002, in preparation
 Knebe, A., & Müller, V. 2000, *A&A*, 354, 761
 Mazure, A., Katgert, P., den Hartog, R., et al. 1996, *A&A*, 310, 31, Paper II
 Melnick, J., & Sargent, W. L. W. 1977, *ApJ*, 215, 401
 Menanteau, F., Ellis, R. S., Abraham, R. G., Barger, A. J., & Cowie, L. L. 1999, *MNRAS*, 309, 208
 Merrifield, M. R., & Kent, S. M. 1989, *AJ*, 98, 351
 Merritt, D. 1985, *ApJ*, 289, 18
 Mohr, J. J., Geller, M. J., Fabricant, D. G., et al. 1996, *ApJ*, 470, 724
 Moore, B., Lake, G., & Katz, N. 1998, *ApJ*, 495, 139
 Moore, B., Lake, G., Quinn, T., & Stadel, J. 1999, *MNRAS*, 304, 465
 Moss, C., & Dickens, R. J. 1977, *MNRAS*, 178, 701
 Oemler, A. Jr. 1974, *ApJ*, 194, 1
 Okamoto, T., & Nagashima, M. 2001, *ApJ*, 547, 109
 Peacock, J. A. 1983, *MNRAS*, 202, 615
 Pence, W. 1976, *ApJ*, 203, 39
 Poggianti, B., Smail, I., Dressler, A., et al. 1999, *ApJ*, 518, 576
 Postman, M., & Geller, M. 1984, *ApJ*, 281, 95
 Poulain, P., & Nieto, J.-L. 1994, *A&AS*, 103, 573
 Quilis, V., Moore, B., & Bower, R. 2001, *Science*, 288, 1617
 Rood, H. J., & Turnrose, B. E. 1968, *ApJ*, 152, 1057
 Rood, H. J., Page, T. L., Kintner, E. C., & King, I. R. 1972, *ApJ*, 175, 627
 Sandage, A. 1973, *ApJ*, 183, 711
 Santiago, B. X., & Strauss, M. A. 1992, *ApJ*, 387, 9
 Silverman, B. W. 1986, *Density estimation for statistics and data analysis* (Chapman and Hall, London), *ApJS*, 110, 213
 Sodré, L. Jr., Capelato, H. V., Steiner, J. E., & Mazure, A. 1989, *AJ*, 97, 1279
 Solanes, J. M., Manrique, A., García-Gómez, C., Giovanelli, R., & Haynes, M. P. 2001, *ApJ*, 548, 97
 Stein, P. 1997, *A&A*, 317, 670
 Tammann, G. A. 1972, *A&A*, 21, 355
 Thomas, P. A., Muanwong, O., Pearce, F. R., et al. 2001, *MNRAS*, 324, 450
 Thomas, T. 2002, *A&A*, submitted, Paper VIII
 Thomas, T., Hartendorp, M., & Katgert, P. 2002, *A&A*, submitted, Paper IX
 Yepes, G., Dominguez-Tenreiro, R., & Del Pozzo-Sanz, R. 1991, *ApJ*, 373, 336
 Whitmore, B. C., & Gilmore, D. M. 1991, *ApJ*, 367, 94
 Whitmore, B. C., Gilmore, D. M., & Jones, C. 1993, *ApJ*, 407, 489